$W_2Cl_4(NR_2)_2(PR'_3)_2$ Molecules. 8. Synthesis and Structural Characterization of Both *Cis* Isomers of Stoichiometry $W_2Cl_4(NHR)_2(PMe_3)_2$, R = Et, Pr^n, and Bu^n. Direct Evidence Favoring an Internal Flip Mechanism for *Cis*−*Trans* Isomerization

F. Albert Cotton,* Evgeny V. Dikarev, and Wai-Yeung Wong

Department of Chemistry and Laboratory for Molecular Structure and Bonding, Texas A&M University, College Station, Texas 77843-3255

Received January 10, 1997⊗

The triply-bonded ditungsten(III) complexes of stoichiometry $W_2Cl_4(NHR)_2(PMe_3)_2$ (R = Et, Pr^n, Bu^n) are formed by a two-step, one-pot, synthesis from the reaction of $W_2Cl_6(THF)_4$ with the appropriate alkylamines NH_2R (R = Et, Pr^n, Bu^n), followed by phosphine substitution. The dinuclear species $W_2Cl_4(NHR)_2(NH_2R)_2$ are the probable intermediate complexes for such reactions. In each case, three isomeric forms have been detected in solution by $^{31}P\{^1H\}$NMR spectroscopy, and they are formulated as the *trans* isomers and the two types of *cis* isomers possessing C_i and C_2 symmetries. It has also been shown that the *trans* isomers are the initial (kinetic) products irrespective of the R group. The X-ray crystallographic characterization of the C_i isomer of *cis*-$W_2Cl_4(NHEt)_2(PMe_3)_2$ (**1**), the C_2 isomer of *cis*-$W_2Cl_4(NHPr^n)_2(PMe_3)_2$ (**2**), and the C_2 isomer of *cis*-$W_2Cl_4(NHBu^n)_2(PMe_3)_2$ (**3a**,**b**) has been accomplished. Crystallographic data are as follows: compound **1**, triclinic space group $P\bar{1}$, $a = 7.4366(2)$ Å, $b = 8.8618(6)$ Å, $c = 9.352(1)$ Å, $\alpha = 105.262(6)°$, $\beta = 109.20(1)°$, $\gamma = 94.423(9)°$, $Z = 1$; compound **2**, monoclinic space group $I2/a$, $a = 13.1268(8)$ Å, $b = 10.871(1)$ Å, $c = 17.106(1)$ Å, $\beta = 92.872(5)°$, $Z = 4$; compound **3a**, monoclinic space group $P2_1/c$, $a = 22.058(9)$ Å, $b = 8.562(1)$ Å, $c = 29.768(8)$ Å, $\beta = 105.642(1)°$, $Z = 8$; compound **3b**, $P2_1/n$, $a = 8.5429(8)$ Å, $b = 18.393(2)$ Å, $c = 16.957(3)$ Å, $\beta = 90.264(5)°$, $Z = 4$. Complex **1** is the first structurally characterized compound with a $W_2Cl_4N_2P_2$ core of C_i symmetry. The midpoint of the W−W unit in **1** resides on an inversion center and compound **1** is therefore nonchiral. For **2** and **3** (**3a**,**b**), the molecules are chiral since each has only C_2 symmetry. The W−W distances for **1**, **2**, **3a**, and **3b** are 2.3066(6), 2.3170(6), 2.3162(9), and 2.3147(5) Å, respectively. In these molecules there are two intramolecular hydrogen bonds across the W−W triple bond, thus ensuring an essentially eclipsed geometry in each case. Each of them has the P and N atoms on each W atom cis to each other. The observation and, in one case, **1**, the isolation of the unprecedented *cis* isomers of C_i symmetry provide support for our earlier proposal that the isomerization processes occur by an "internal flip" of the W_2 unit within the quasi-cubic set of coordinated ligand atoms.

Introduction

Earlier work from this laboratory showed that *cis* and *trans* isomers occur for $W_2Cl_4(NHR)_2(PR'_3)_2$ molecules, and the interconversion process has been studied in detail.[1] A unimolecular mechanism involving an internal flip of the W_2 unit within the ligand cage of eight ligand atoms was proposed.[1] However, in none of the systems studied so far was a second possible *cis* isomer of C_i symmetry observed, and the question of why this isomer had not been seen remained unanswered. A demonstration of the existence of this isomer is particularly crucial to the internal flip proposal since it could readily be formed by a mechanism entailing one internal flip step only.[1a]

In an attempt to obtain more direct evidence to support our mechanistic proposal, detailed studies concerning variations of the sizes of the coordinated ligands have been carried out.[1] Particularly promising to us in the initial stage of this study was the observation of a new $^{31}P\{^1H\}$NMR signal (shown later to arise from the unknown *cis* isomer) when the less bulky ligand, namely, *n*-butylamide, was used. We therefore resorted to using those amido ligands bearing some simple *n*-alkyl substituents ranging from Bu^n to the least sterically bulky Me groups in the hope that the elusive *cis* isomer could be isolated. Experiments reported here have confirmed our expectations.

Herein, we report the preparation, $^{31}P\{^1H\}$NMR spectroscopic studies, and structural characterization of two types of *cis* isomers having stoichiometry $W_2Cl_4(NHR)_2(PMe_3)_2$ (R = Et, Pr^n, Bu^n). These isomers possess C_i and C_2 symmetries, which can be designated, respectively, as *cis*(C_i) and *cis*(C_2). The relevance of the complexes *cis*-$W_2Cl_4(NHR)_2(PMe_3)_2$ of C_i symmetry to the suggested internal flip mechanism in the *cis*−*trans* isomerizations of $W_2Cl_4(NHR)_2(PR'_3)_2$ molecules will be discussed.

Experimental Section

General Procedures. All the syntheses and purifications were carried out under N_2 or argon in standard Schlenkware. All solvents used were freshly distilled under N_2 from suitable drying reagents. Chemicals were purchased from the following commercial sources and used as received: PMe_3, Strem Chemicals; ethylamine (2.0 M solution in THF), *n*-propylamine and *n*-butylamine, Aldrich, Inc. Toluene-d_8 and benzene-d_6 were obtained from Cambridge Isotope Laboratories and dried over 3 Å molecular sieves. WCl_4 was synthesized by refluxing WCl_6 and $W(CO)_6$ in chlorobenzene.[2] A general literature method was used to prepare $W_2Cl_6(THF)_4$ using Na−Hg as the reducing agent.[3]

Preparation of $W_2Cl_4(NHEt)_2(PMe_3)_2$. (i) Ethylamine (2.0 M in THF, 2.31 mL, 4.62 mmol) was added by syringe to a stirred solution

---

⊗ Abstract published in *Advance ACS Abstracts,* May 15, 1997.

(1) (a) Chen, H.; Cotton, F. A.; Yao, Z. *Inorg. Chem.* **1994**, *33*, 4255. (b) Part 7: Cotton, F. A.; Dikarev, E. V.; Wong, W. Y. *Inorg. Chem.*, in press.

(2) Schrock, R. R.; Sturgeoff, L. G.; Sharp, P. R. *Inorg. Chem.* **1983**, *22*, 2801.

(3) (a) Chisholm, M. H.; Eichhorn, B. W.; Folting, K.; Huffman, J. C.; Ontiveros, C. D.; Streib, W. E.; Van Der Sluys, W. G. *Inorg. Chem.* **1987**, *26*, 3182. (b) Sharp, P. R.; Schrock, R. R. *J. Am. Chem. Soc.* **1980**, *102*, 1430.

S0020-1669(97)00036-0 CCC: $14.00

Table 1. Crystallographic Data for *cis*-$W_2Cl_4(NHEt)_2(PMe_3)_2$ (**1**), *cis*-$W_2Cl_4(NHPr^n)_2(PMe_3)_2$ (**2**), and *cis*-$W_2Cl_4(NHBu^n)_2(PMe_3)_2$ (**3a,b**)

	1	**2**	**3a**	**3b**
formula	$W_2Cl_4P_2C_{10}H_{30}N_2$	$W_2Cl_4P_2C_{12}H_{34}N_2$	$W_2Cl_4P_2C_{14}H_{38}N_2$	$W_2Cl_4P_2C_{14}H_{38}N_2$
fw	749.80	777.85	805.90	805.90
space group	$P\bar{1}$ (No. 2)	I2/*a* (No. 15)	P2$_1$/*c* (No. 14)	P2$_1$/*n* (No. 14)
a, Å	7.4366(2)	13.1268(8)	22.058(9)	8.5429(8)
b, Å	8.8618(6)	10.871(1)	8.562(1)	18.393(2)
c, Å	9.352(1)	17.106(1)	29.768(8)	16.957(3)
α, deg	105.262(6)	90.0	90.0	90.0
β, deg	109.20(1)	92.872(5)	105.642(1)	90.264(5)
γ, deg	94.423(9)	90.0	90.0	90.0
V, Å^3	552.37(7)	2438.0(3)	5414(3)	2664.4(6)
Z	1	4	8	4
ρ_{calc}, g/cm^3	2.254	2.119	1.978	2.009
μ, mm^{-1}	11.026	9.997	9.008	9.151
radiation (λ, Å)	Mo Kα (0.710 73)	Mo Kα (0.710 73)	Mo Kα (0.710 73)	Mo Kα (0.710 73)
temp, °C	−60	−60	−60	−60
$R1$,[a] w$R2$[b] [$I > \sigma 2(I)$]	0.031, 0.077	0.038, 0.089	0.060, 0.132	0.041, 0.097
$R1$,[a] w$R2$[b] (all data)	0.033, 0.084	0.045, 0.093	0.118, 0.153	0.060, 0.105

[a] $R1 = \Sigma||F_o| - |F_c|/\Sigma|F_o|$. [b] $wR2 = [\Sigma[w(F_o2 - F_c2)^2]/\Sigma[w(F_o2)^2]]^{1/2}$.

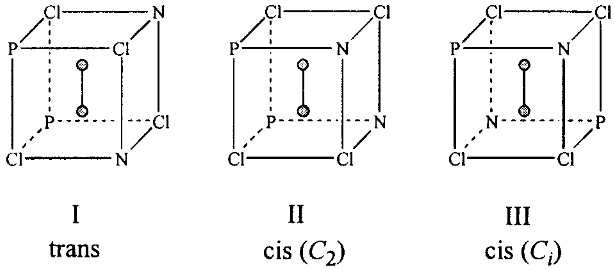

Figure 1. *Trans* and two possible *cis* isomers of $W_2Cl_4N_2P_2$ molecules.

Table 2. $^{31}P\{^1H\}$NMR Data for the *Trans* and Two Types of *Cis* Isomers of the $W_2Cl_4(NHR)_2(PMe_3)_2$ Compounds at Room Temperature

	trans		*cis*(C_2)			*cis*(C_i)		
R	^{31}P shift[a]	$^1J_{W-P}$[b]	^{31}P shift	$^1J_{W-P}$	$^3J_{P-P}$	^{31}P shift	$^1J_{W-P}$	$^3J_{P-P}$
Et	−4.77	115	−1.01	308	5.0	3.10	340	15.5
Pr^n	−4.76	115	−1.01	309	4.9	3.12	340	15.9
Bu^n	−4.79	113	−1.04	308	4.9	3.17	338	15.0

[a] Relative to 85% H_3PO_4/D_2O in C_6D_6/THF. [b] In Hz.

of $W_2Cl_6(THF)_4$ prepared by reduction of WCl_4 (0.50 g, 1.54 mmol) with 1 equiv of Na−Hg (0.4%) in tetrahydrofuran (15 mL). The initial greenish-yellow color gradually turned to brown over 30 min, and the mixture was then stirred for 12 h to ensure completion of the reaction. The solution was freed from both Hg and NaCl by filtration through a Celite column. To this filtrate was added an excess of PMe_3 (0.16 mL) whereupon the solution turned dark brown in color. *In situ* monitoring by $^{31}P\{^1H\}$NMR spectroscopy of a sample of the mixture at the early stage of the experiment (within 10 min) revealed the presence of *trans*-$W_2Cl_4(NHEt)_2(PMe_3)_2$ only at room temperature. As time went by, a signal arising from the previously unknown *cis* isomer of C_i symmetry started to appear and eventually all three isomers (*trans*, *cis*(C_i), and *cis*(C_2)) were found to exist simultaneously in solution. After about 30 min of stirring, the solvent and other volatile components were removed in vacuum to leave a dark brown residue, which was then extracted with toluene (20 mL). The filtrate was reduced in volume to one-third and stored overnight at −20 °C. A small quantity of tiny red-brown crystals of **1** (29 mg, 5% based on WCl_4) was deposited at the base of the Schlenk tube. One of them was subjected to X-ray structural analysis. Attempts to isolate and crystallize the other two isomers were unsuccessful so far, and no attempts were made to optimize the yield of **1** in this reaction. It was found that a solution of *cis*-$W_2Cl_4(NHEt)_2(PMe_3)_2$ of C_i symmetry was susceptible to decomposition even at low temperature when attempts were made to crystallize this compound.

For the *trans* isomer, $^{31}P\{^1H\}$NMR (C_6D_6/THF, 1/3, 19 °C): δ −4.77 (s, $^1J_{W-P} = 115$ Hz).

For **1**, $^{31}P\{^1H\}$NMR (C_6D_6/THF, 1/3, 19 °C): δ 3.10 (s, $^1J_{W-P} =$ 340 Hz, $^3J_{P-P} = 15.5$ Hz).

For the *cis*(C_2) isomer, $^{31}P\{^1H\}$NMR (C_6D_6/THF, 1/3, 19 °C): δ −1.01 (s, $^1J_{W-P} = 308$ Hz, $^3J_{P-P} = 5.0$ Hz).

Preparation of $W_2Cl_4(NHPr^n)_2(PMe_3)_2$. (ii) To the tetrahydrofuran solution (15 mL) of $W_2Cl_6(THF)_4$ (from 0.50 g of WCl_4), *n*-propylamine (0.38 mL, 4.62 mmol) was added via syringe and the color of the solution became brown within 1 h. The reaction was terminated after 12 h of stirring, and both the NaCl which formed and the mercury residue were removed by filtering the reaction mixture through Celite. Excess PMe_3 (0.16 mL) was then added to the filtrate. This solution contained a mixture of three distinct isomers (*trans* and two types of *cis* isomers) within 30 min of stirring as evidenced by the ^{31}P NMR. The reaction mixture was then stirred for an additional $^1/_2$ h. After evaporation of the solvents under vacuum, the residue was extracted with warm hexanes (10 mL) to give a pale brown solution from which tiny red-brown crystals of **2** formed after 1 day at room temperature. The remaining residue was then dissolved in toluene (15 mL), and well-formed red crystals of **2** of X-ray quality were obtained by hexanes/toluene layering at room temperature. Yield: 0.25 g (42% based on WCl_4). No crystals were obtained for the remaining two isomers because of their ready transformation to compound **2**.

For the *trans* isomer, $^{31}P\{^1H\}$NMR (C_6D_6/THF, 1/3, 19 °C): δ −4.76 (s, $^1J_{W-P} = 115$ Hz).

For the *cis*(C_i) isomer, $^{31}P\{^1H\}$NMR (C_6D_6/THF, 1/3, 19 °C): δ 3.12 (s, $^1J_{W-P} = 340$ Hz, $^3J_{P-P} = 15.9$ Hz).

For **2**, IR (cm^{-1}): 3227 (ms), 3202 (ms), 1425 (ms), 1416 (ms), 1355 (ms), 1341 (m), 1321 (vw), 1300 (m), 1288 (s), 1279 (ms), 1262 (w), 1216 (m), 1091 (ms), 1082 (ms), 1067 (m), 1056 (w), 1025 (vw), 982 (ms), 958 (vs), 897 (vw), 858 (m), 846 (m), 791 (m), 746 (s), 738 (s), 694 (vw), 675 (w), 641 (w).

^{1}H NMR (C_6D_6, 24 °C): δ 0.70 (t, $J = 7.4$ Hz, 6H, $NCH_2CH_2CH_3$), 1.30−1.42 (m, 4H, $NCH_2CH_2CH_3$), 1.37 (d, $J = 9.7$ Hz, 18H, PMe_3), 3.03 (m, 2H, $NCH_2CH_2CH_3$), 3.25 (m, 2H, $NCH_2CH_2CH_3$), 11.72 (m, br, NH).

$^{31}P\{^1H\}$NMR (C_6D_6/THF, 1/3, 19 °C): δ −1.01 (s, $^1J_{W-P} = 309$ Hz, $^3J_{P-P} = 4.9$ Hz).

FAB/DIP MS (NBA, CH_2Cl_2): *m/z* 778 ([M]$^+$), 741 ([M − Cl]$^+$), 718 ([M − NHPr^n]$^+$), 700 ([M − PMe$_3$]$^+$), 680 ([M − Cl − NHPr^n]$^+$), 665 ([M − Cl − PMe$_3$]$^+$), 644 ([M − 2Cl − NHPr^n]$^+$), 624 ([M − 2PMe$_3$]$^+$), 604 ([M − Cl − NHPr^n − PMe$_3$]$^+$).

Preparation of $W_2Cl_4(NHBu^n)_2(PMe_3)_2$. (iii) The synthesis of $W_2Cl_4(NHBu^n)_2(PMe_3)_2$ followed a course similar to that for (i) and (ii). Upon addition of *n*-butylamine (0.46 mL, 4.62 mmol) to a THF solution (15 mL) of $W_2Cl_6(THF)_4$ (from 0.50 g WCl_4) and subsequent PMe_3 substitution (0.16 mL), the $^{31}P\{^1H\}$NMR spectrum initially showed the formation of the *trans* isomer in solution, followed by the building up of the two *cis* isomers. Stirring was continued for about 1 h, after which all the volatile components of the mixture were removed under reduced pressure. Extraction of the dark brown residue with hot hexanes (25 mL) afforded a brown solution. This was left undisturbed

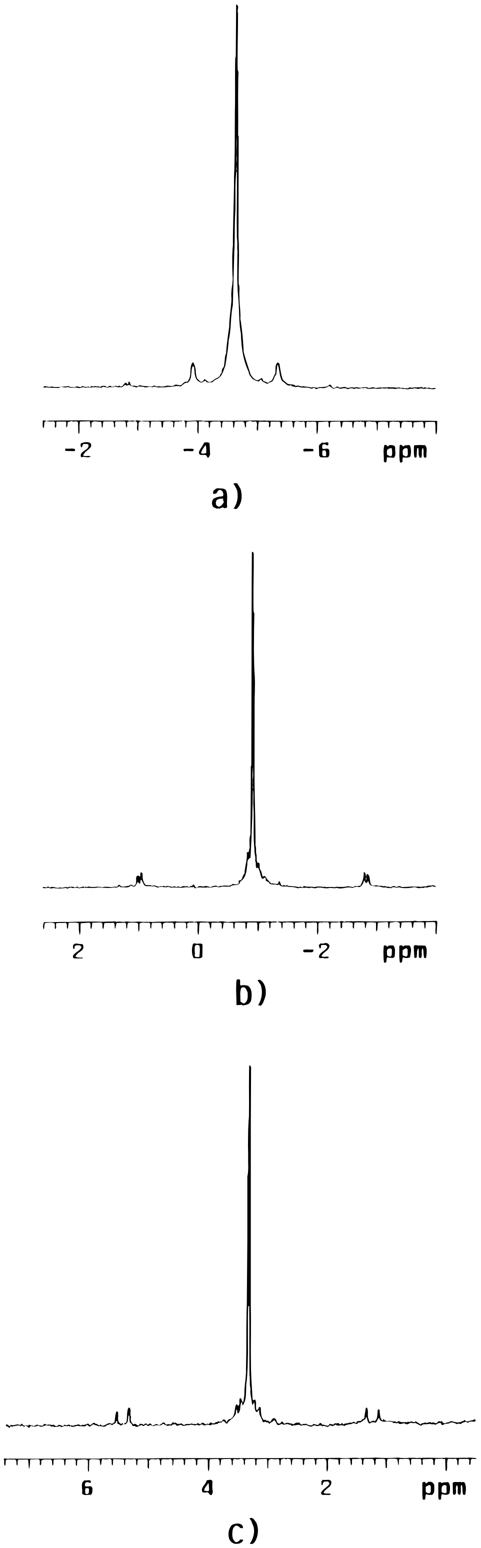

Figure 2. $^{31}P\{^1H\}$NMR spectra of (a) *trans*-, (b) *cis*(C_2)-, and (c) *cis*(C_i)-$W_2Cl_4(NHPr^n)_2(PMe_3)_2$ at room temperature in C_6D_6/THF.

at room temperature for 2 days and produced an abundant crop of red-brown crystals of **3a** (0.23 g, 37% based on WCl_4) with needle morphology. Crystals grown in this way have been used for other studies including X-ray crystallography. When we approached the preparation of $W_2Cl_4(NHBu^n)_2(PMe_3)_2$ compounds using a hexanes extract of the intermediate complex, presumably $W_2Cl_4(NHBu^n)_2(NH_2Bu^n)_2$, another crystalline form of the compound (**3b**) was fortuitously obtained in low yield (30 mg, 5% based on WCl_4) as deep red blocks from a concentrated hexanes solution.

For the *trans* isomer, $^{31}P\{^1H\}$NMR data (C_6D_6/THF, 1/3, 19 °C): δ −4.79 (s, $^1J_{W-P} = 113$ Hz).

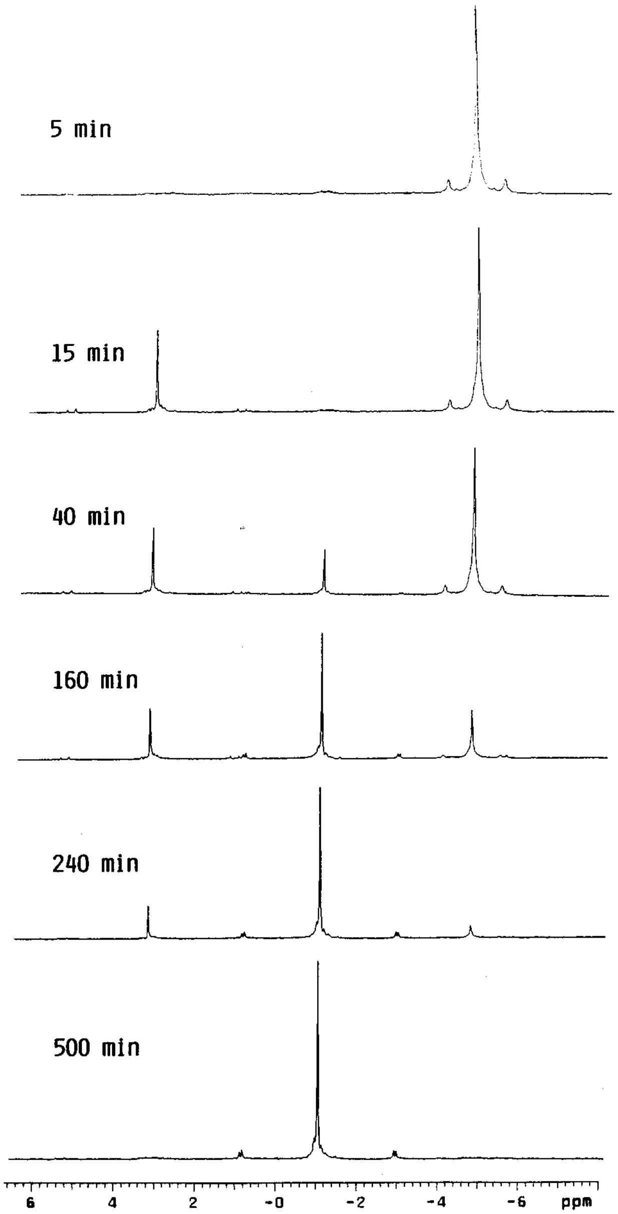

Figure 3. In *situ* $^{31}P\{^1H\}$NMR spectra of $W_2Cl_4(NHPr^n)_2(PMe_3)_2$ at different times under ambient conditions.

For the *cis*(C_i) isomer, $^{31}P\{^1H\}$NMR (C_6D_6/THF, 1/3, 19 °C): δ 3.19 (s, $^1J_{W-P} = 338$ Hz, $^3J_{P-P} = 15.0$ Hz).

For **3**, IR (cm^{-1}): 3219 (w), 1416 (w), 1365 (w), 1302 (w), 1286 (w), 1261 (vs), 1198 (w), 1098 (vs), 1021 (vs), 958 (ms), 863 (m), 800 (vs), 738 (w).

^{1}H NMR (C_6D_6, 24 °C): δ 0.72 (t, $J = 7.2$ Hz, 6H, $N(CH_2)_3CH_3$), 1.16 (m, 8H, $NCH_2(CH_2)_2CH_3$, 1.38 (d, $J = 9.6$ Hz, 18H, PMe_3), 3.13 (m, 2H, $NCH_2(CH_2)_2CH_3$), 3.30 (m, 2H, $NCH_2(CH_2)_2CH_3$), 11.72 (br, 2H, NH).

$^{31}P\{^1H\}$NMR (C_6D_6/THF, 1/3, 19 °C): δ −1.04 (s, $^1J_{W-P} = 308$ Hz, $^3J_{P-P} = 4.9$ Hz).

FAB/DIP MS (NBA, neat): *m/z* 805 ([M]$^+$), 769 ([M − Cl]$^+$), 731 ([M − PMe$_3$]$^+$ or [M − NHBu^n]$^+$), 693 ([M − Cl − PMe$_3$]$^+$), 654 ([M − 2PMe$_3$]$^+$), 620 ([M − Cl − 2PMe$_3$]$^+$).

Physical Measurements. The IR spectra were recorded on a Perkin-Elmer 16PC FT-IR spectrophotometer using Nujol mulls between KBr plates. ^{1}H NMR spectra were obtained on a Varian XL-200 spectrometer operated at 200 MHz. Resonances were referenced internally to the residual proton impurity in the deuterated solvent. The $^{31}P\{^1H\}$ NMR data were obtained at room temperature on a Varian XL-200 broad band spectrometer operated at 81 MHz and using an internal deuterium lock and 85% H_3PO_4 as an external standard. Positive chemical shifts were measured downfield from H_3PO_4/D_2O. The

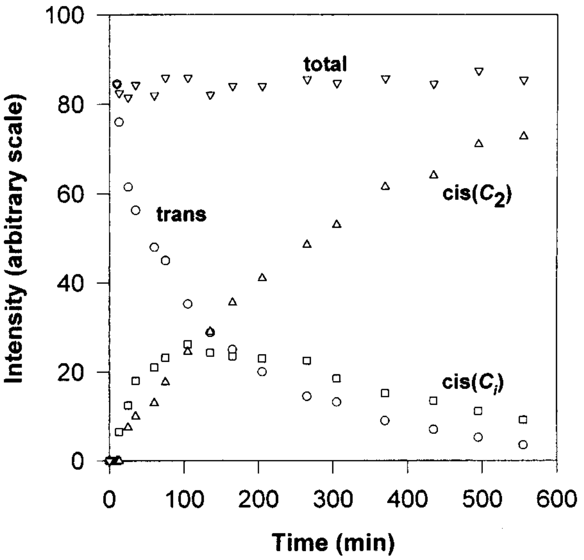

Figure 4. Plot of the intensity of the three isomers of $W_2Cl_4(NHEt)_2(PMe_3)_2$ versus time at room temperature in C_6D_6/THF.

positive FAB/DIP (DIP = direct insertion probe) mass spectra were acquired using a VG Analytical 70S high resolution, double-focusing, sectored (EB) mass spectrometer. Samples for analysis were prepared either by dissolving neat solid compound in *m*-nitrobenzyl alcohol (NBA) matrix or mixing a solution of the compound in CH_2Cl_2 with NBA matrix on the direct insertion probe tip.

Solution $^{31}P\{^1H\}$NMR Study of $W_2Cl_4(NHR)_2(PMe_3)_2$ (R = Et, Pr^n). A 1.5 mL THF solution taken from the $W_2Cl_4(NHR)_2(PMe_3)_2$ reaction mixture, together with 0.5 mL of benzene-d_6, was placed in a 10 mm o.d. NMR sample tube under N_2. The NMR tube was then sealed with a rubber septum. The 81 MHz $^{31}P\{^1H\}$NMR spectra were measured at 19 °C at regular time intervals.

X-ray Crystallographic Procedures. Single crystals of compounds **1**, **2**, **3a,** and **3b** for diffraction experiments were obtained as described in the Experimental Section. In all cases, crystals were mounted on the tip of a quartz fiber with silicone grease and the setup was quickly placed in the cold stream at −60 °C of the Model FR 558-S low-temperature controller. Geometric and intensity data were collected on an Enraf-Nonius FAST diffractometer with an area detector using Mo Kα radiation. Details for data collection have been fully described elsewhere.[4] The cell parameters were obtained from an auto-indexing routine and were refined with about 250 strong reflections. Axial images were used to confirm the Laue group and lattice dimensions. The data were corrected for Lorentz and polarization effects by the MADNES program.[5] All calculations were done on a DEC 3000-800 AXP workstation. The coordinates of tungsten atoms for all of the structures were found in direct-methods *E*-maps using the structure solution program in SHELXTL.[6] A series of alternating least-squares refinements and difference Fourier maps using the SHELXL-93 program[7] led to satisfactory development of the atoms in the coordination spheres of the W atoms. These positions were initially refined with isotropic displacement parameters and then with anisotropic displacement parameters to convergence. Where necessary, the intensity data were corrected for absorption anisotropy effects by the SORTAV program.[8] In each model, hydrogen atoms were included at idealized positions for the calculations of F_c, and the entire model was refined to convergence. Important crystal data pertinent to individual compounds and the structure refinement results are assemblied in Table 1.

***cis*-$W_2Cl_4(NHEt)_2(PMe_3)_2$ (1).** A red-brown needle-shaped crystal with dimensions of 0.05 × 0.05 × 0.13 mm was selected for intensity measurements. Choice of the centrosymmetric space group $P\bar{1}$ revealed the position of the unique W atom and successful refinement of the structure confirmed the choice. No absorption correction was made. Full refinement of 95 parameters led to residuals of $R = 0.031$ (for 1752 reflections with $I > 2\sigma(I)$) and $R = 0.033$ (for all 1831 data). The largest peak in the final difference map was 1.78 e/Å^3, lying 1.01 Å from the W atom.

***cis*-$W_2Cl_4(NHPr^n)_2(PMe_3)_2$ (2).** An orange-red block-shaped crystal of dimensions 0.09 × 0.15 × 0.20 mm was mounted. Indexing based on 249 reflections in the range $18 < 2\theta < 42°$ resulted in unit cell parameters having body-centered monoclinic symmetry. Systematic absences in the data led to the selection of space group $I2/a$. Direct methods revealed the location of the unique W atom W(1) of a dinuclear unit. W(1) and W(1A) atoms are symmetry related. Absorption corrections were applied to the data set. It was found that the carbon atoms in the *n*-propyl groups were disordered over two sites. This disorder was modeled by constraining the displacement parameters to be equal and restraining the chemically equivalent bonds to be approximately equal. The site occupancy factors were allowed to vary but were constrained so that the sum was equal to 1. The resulting model yielded reasonable bond distances and angles. Final anisotropic refinement of 84 parameters resulted in $R = 0.038$ (for 1811 reflections with $I > 2\sigma(I)$), and $R = 0.045$ (for all 2039 independent reflections). The final difference map was essentially featureless, the largest peaks being associated with the W atoms.

***cis*-$W_2Cl_4(NHBu^n)_2(PMe_3)_2$ (3a).** The red crystal selected was needle-shaped with dimensions 0.05 × 0.08 × 0.60 mm. The crystal was shown to belong to the primitive monoclinic system, and systematic absences unambiguously assigned the space group as $P2_1/c$. Direct methods provided the positions of four W atoms corresponding to the two independent ditungsten units in the asymmetric unit. After the successful development of the structure and anisotropic refinement of heavy atoms, difference Fourier maps showed two peaks close to W(1) and W(2), and the bond distances and bond angles indicated that they were a secondary pair of W atoms. The occupancy for the main orientation, W(1)−W(2), was 94.4%, and the secondary orientation W(5)−W(6) has 5.6% occupancy. There was no disorder in the W(3)−W(4) dinuclear unit. In addition, both *n*-butyl chains were found to be disordered over two positions and a strategy similar to that for compound **2** was used for modeling the disorder. Corrections for absorption were made. Final least-squares refinement of 419 parameters converged with $R = 0.060$ (for 5260 reflections with $I > 2\sigma(I)$) and $R = 0.118$ (for all 9207 data). The final difference electron density map had no significant features other than several small peaks close to the W atoms.

***cis*-$W_2Cl_4(NHBu^n)_2(PMe_3)_2$ (3b).** A red block of size 0.10 × 0.25 × 0.30 mm was used for diffraction studies. Examination of the systematic absences led to the space group $P2_1/n$. Only one ditungsten unit was found in the asymmetric unit. Absorption corrections were applied to the intensity data. For 4497 unique reflections, the refinement of 221 parameters converged with a final agreement at $R = 0.060$. For the 3538 reflections with $I > 2\sigma(I)$, $R = 0.041$. No disorder or other problems arose. The largest peak in the final difference Fourier map had an electron density of 1.49 e/Å^3 and was located near the W atom.

Results and Discussion

Syntheses and Properties. The synthesis of $W_2Cl_4(NHR)_2(PMe_3)_2$ (R = Et, Pr^n, Bu^n) proceeds straightforwardly by treatment of $W_2Cl_4(NHR)_2(NH_2R)_2$ (R = Et, Pr^n, Bu^n) with an excess of PMe_3 at ambient temperature. It was found that the *trans* isomers of $W_2Cl_4(NHR)_2(PMe_3)_2$ (type I in Figure 1) are the initial products in each case. They readily isomerize in solution to form first the *cis* isomer of C_i symmetry (type III, Figure 1) and finally the thermodynamically favored *cis* isomer of C_2 symmetry (type II). Thus, the reason that we have not been able to isolate the *trans* isomers in any of the systems

---

(4) Cotton, F. A.; Dikarev, E. V.; Wong, W. Y. *Inorg. Chem.* **1997**, *36*, 80.

(5) Pflugrath, J.; Messerschmitt, A. MADNES, Munich Area Detector (New EEC) System, version EEC 11/9/89, with enhancements by Enraf-Nonius Corp., Delft, The Netherlands. A description of MADNES appears in: Messerschmitt, A.; Plfugrath, J. *J. Appl. Crystallogr.* **1987**, *20*, 306.

(6) SHELXTL V. 5, Siemens Industrial Automation Inc., 1994.

(7) Sheldrick, G. M. *Crystallographic Computing 6*; Flack, H. D., Parkanyi, L., Simon, K., Eds.; Oxford University Press: Oxford, U.K., 1993; p 111.

(8) Blessing, R. H. *Acta Crystallogr.* **1995**, *A51*, 33.

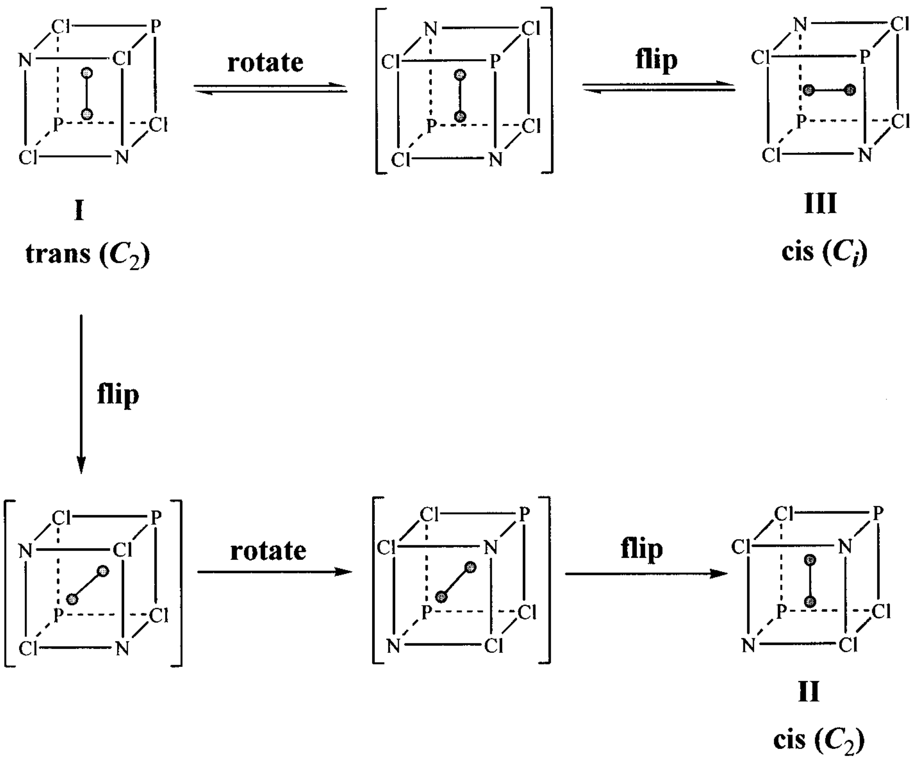

Figure 5. Diagram depicting the three isomeric $W_2Cl_4(NHR)_2(PR'_3)_2$ molecules in a schematic way and showing the possible internal flip steps that can be considered.

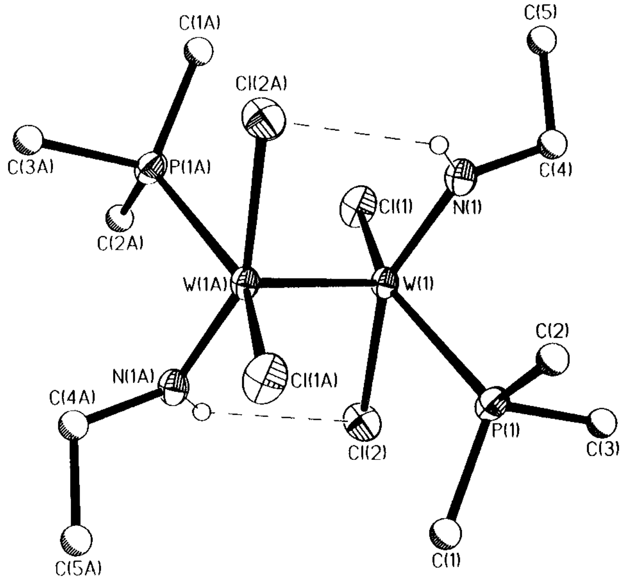

Figure 6. Perspective drawing of *cis*-$W_2Cl_4(NHEt)_2(PMe_3)_2$ (**1**) of C_i symmetry. Atoms are represented by thermal ellipsoids at the 40% probability level. Carbon atoms are shown as spheres of arbitrary radius. Two hydrogen bonds N−H···Cl are shown as dashed lines.

reported here can be understood. On the other hand, an unexpected observation is the decrease in stability of these complexes as the sizes of the amido substituents become progressively smaller. Some consequences of this are the relatively low yield of *cis*-$W_2Cl_4(NHEt)_2(PMe_3)_2$ (**1**) and the facile decomposition of the thermodynamic product (i.e. *cis* isomer of C_2 symmetry) in solution. We also found that similar compounds could not be isolated in the case of $MeNH_2$ and only some insoluble polymeric black solid was obtained.

Compounds **1**−**3** exhibit fair solubility in toluene and benzene, but they are rather unstable in CH_2Cl_2 solutions. In the solid state, they appear to be air stable for short periods of time. However, a significant amount of $WOCl_2(PMe_3)_3$[9] as identified by $^{31}P\{^1H\}$NMR formed when solutions of these compounds were exposed to air.

A useful spectroscopic probe of the presence of NHR groups in these compounds is provided by the appearance of ν(NH) modes in the IR spectra of **2** and **3** at frequencies characteristic of a NHR ligand. Further evidence for this is found in the ^1H NMR spectra which show broad proton resonances at δ 11.72 for **2** and **3**. The ^1H NMR resonances for **2** and **3** are quite similar in that they exhibit a series of multiplets in the range δ 0.70−3.30 for the aliphatic protons and a doublet for the PMe_3 groups at about δ 1.38.

$^{31}P\{^1H\}$NMR and Isomerization Studies. The compounds $W_2Cl_4(NHR)_2(PMe_3)_2$ are diamagnetic as evidenced by their sharp and unshifted ^{31}P NMR spectra. The data are given in Table 2. The $^{31}P\{^1H\}$ NMR spectrum of each isomeric species reveals a single resonance shifted well downfield from that of the free PMe_3 ligand, and thus the phosphines are chemically equivalent. The identities of the three isomeric types of ditungsten complexes observed in this study are readily established by their characteristic $^{31}P\{^1H\}$ NMR spectra. As expected for ABX ($PP^{183}W$) systems in those previously known isomeric types (I and II)[1], both the *trans* isomers (Figure 2a) and the *cis* isomers of C_2 symmetry (Figure 2b) give strong central signals accompanied by weak ^{183}W satellites. In the latter case, the appearance of the satellites as doublets is particularly useful in distinguishing these isomers from their corresponding *trans* counterparts. In the present work, a new signal arose in the $^{31}P\{^1H\}$NMR spectrum of each reaction mixture and is attributed to the remaining possible *cis* isomers of C_i symmetry (type III) (Figure 2c), on the basis of the observed $^1J_{W-P}$ and $^3J_{P-P}$ values characteristic of *cis* isomers. This has been confirmed by an X-ray structural study of *cis*-$W_2Cl_4(NHEt)_2(PMe_3)_2$ (*vide infra*). The $^1J_{W-P}$ values of 340 Hz for the *cis* isomers of C_i symmetry are slightly larger than those due to the other *cis* isomers of C_2

---

(9) Chiu, K. W.; Lyons, D.; Wilkinson, G. *Polyhedron* **1983**, *2*, 803.

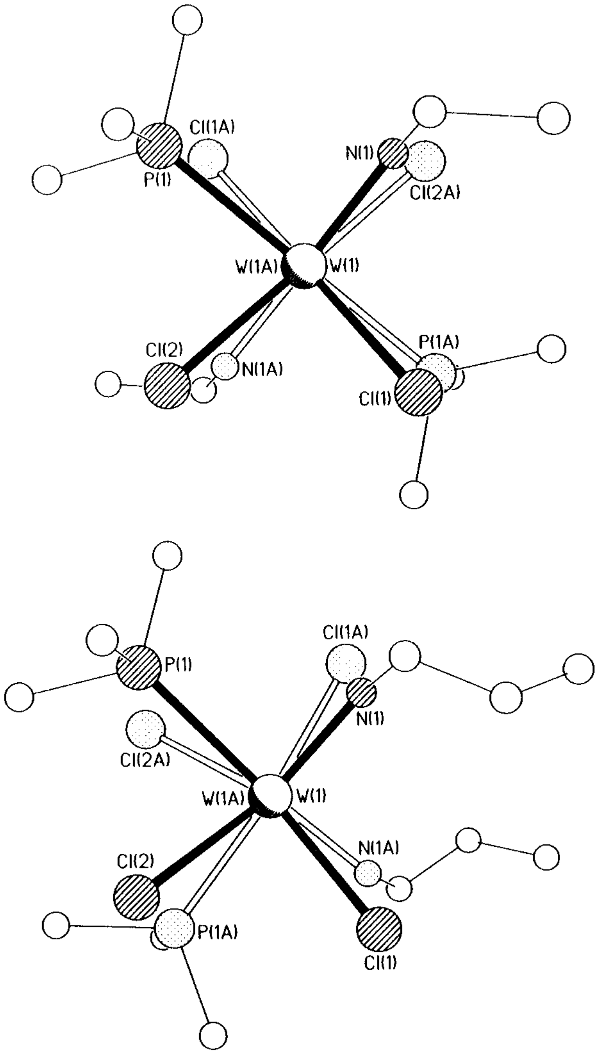

Figure 7. Views of (a, top) the C_i *cis*-$W_2Cl_4(NHEt)_2(PMe_3)_2$ (**1**) and (b, bottom) the C_2 *cis*-$W_2Cl_4(NHPr^n)_2(PMe_3)_2$ (**2**) molecules directly down the W−W axis. For clarity, carbon atoms are not labeled.

symmetry (about 300 Hz) and considerably larger than those in *trans* isomers (about 110 Hz). It is quite obvious that the ^{31}P NMR parameters (δ and J values) for each specific isomer are relatively insensitive to the sizes of the R groups in the amido ligands.

$^{31}P\{^1H\}$NMR studies showed that the initial *trans* products of $W_2Cl_4(NHR)_2(PMe_3)_2$ (R = Et, Pr^n, Bu^n) rapidly undergo isomerization in solution to the two corresponding *cis* isomers (C_i and C_2 symmetries) at room temperature. Accordingly, we monitored this process for $W_2Cl_4(NHPr^n)_2(PMe_3)_2$ spectroscopically over time with the results shown in Figure 3. Initially, only the *trans* isomer was observed. After about 40 min, three isomers were present at the same time in solution. It was found that the final spectrum in the sequence was essentially identical with that of the pure *cis*(C_2) isomer. In a separate experiment for $W_2Cl_4(NHEt)_2(PMe_3)_2$, when intensities of a mixture of three distinct isomers are plotted, the results are depicted in Figure 4. On the other hand, experimental observations suggest that the rates of isomerization to the thermodynamically favored *cis*(C_2) isomers essentially follow the order $Bu^n > Pr^n >$ Et, which is in accord with the fact that the *cis*(C_i) isomer can only be isolated for R = Et.

Figure 5 shows schematic representations of the three isomeric molecules I−III, and indicates all possible conversion pathways that might be considered in an internal flip mechanism. It is clear that there is only one *trans* isomer with C_2 symmetry in this system. In our previous studies of $W_2Cl_4(NHCMe_3)_2(PR_3)_2$ molecules, only isomers of types I and II were known to exist[1a] and the conversion I → II was directly observed which involves two flip steps. This observation is a bit surprising to us since we believe that the process I → III, which entails one internal flip only, should be competitive in rate or even more favorable than the I → II conversion pathway. With the use of the least sterically bulky amido ligands in the present system, we have actually observed the process I → III and found that appreciable amounts of III can exist at intermediate time periods. The process III → II then takes over as the final, thermodynamic product in each case. It should be noted that, in Figure 5, none of the three intermediate species in brackets is believed to be isolable.

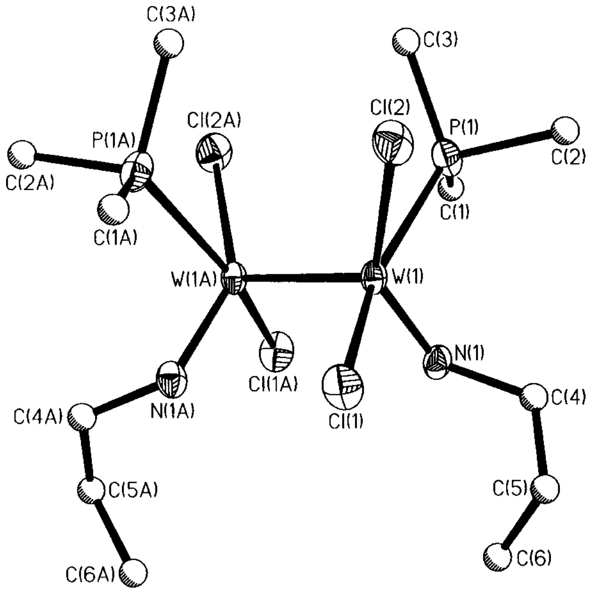

Figure 8. Perspective drawing of the C_2 *cis*-$W_2Cl_4(NHPr^n)_2(PMe_3)_2$ (**2**) molecule. Only the major orientation of the carbon atoms is shown. Atoms are represented by thermal ellipsoids at the 40% probability level. Carbon atoms are shown as spheres of arbitrary radius.

For the $W_2Cl_4(NHR)_2(PMe_3)_2$ compounds with smaller R groups, namely, Et, Pr^n and Bu^n, the final state of equilibrium in solution leaves only the *cis*(C_2) isomers in detectable (by NMR) amounts. This contrasts with the cases where R is very bulky, i.e. Bu^t [1a] and Cy,[1b] where the equilibrium mixture contains both *trans* and *cis*(C_2) isomers. Clearly, the relative thermodynamic stabilities of the three isomers are quite sensitive to the steric effects of the R groups. It *may* be possible to account for this theoretically, and efforts to do so are underway.[10]

The isomerization scheme shown in Figure 5 is in accord with the fact that the *cis*(C_i) isomer can initially form more rapidly than the *cis*(C_2) isomer since the activation energy may well be smaller for *trans* → *cis*(C_i) than for *trans* → *cis*(C_2). In the end, however, all *trans* and *cis*(C_i) become undetectable owing to the greater stability of *cis*(C_2).

Structural Results. Complex **1** crystallizes in space group $P\bar{1}$ with the molecule possessing an inversion center at the midpoint of the W−W vector. The molecule is thus nonchiral because it has C_i symmetry. Half of the molecule constitutes the asymmetric unit, and there is one complete molecule in the unit cell. The molecular structure of **1** is depicted in Figure 6, and selected bond distances and angles are listed in Table 3. Although examples of structures of *cis*-$W_2Cl_4(NHR)_2(PR'_3)_2$ molecules having C_2 symmetry are known in the literature,[11]

---

[10] Feng, X. Private communication.

Table 3. Selected Bond Distances (Å) and Angles (deg) and Torsion Angles (deg) for *cis*-$\mathrm{W_2Cl_4(NHEt)_2(PMe_3)_2}$ (**1**)

W(1)−W(1A)	2.3066(6)	W(1)−P(1)	2.497(2)
W(1)−N(1)	1.912(7)	W(1)−Cl(1)	2.398(2)
W(1)−Cl(2)	2.432(2)		
P(1)−W(1)−N(1)	87.5(2)	P(1)−W(1)−Cl(1)	148.80(7)
P(1)−W(1)−Cl(2)	80.18(8)	N(1)−W(1)−Cl(1)	95.1(2)
N(1)−W(1)−Cl(2)	155.6(2)	Cl(1)−W(1)−Cl(2)	85.07(8)
W(1A)−W(1)−P(1)	95.69(5)	W(1A)−W(1)−N(1)	99.2(2)
W(1A)−W(1)−Cl(1)	114.43(5)	W(1A)−W(1)−Cl(2)	102.95(5)
P(1)−W(1)−W(1A)−Cl(1A)	8.37(9)	N(1)−W(1)−W(1A)−Cl(2A)	10.4(2)
Cl(1)−W(1)−W(1A)−P(1A)	−8.37(9)	Cl(2)−W(1)−W(1A)−N(1A)	−10.4(2)

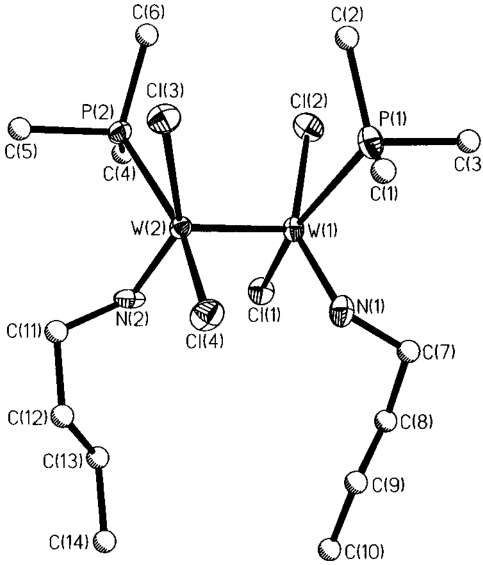

Figure 9. Perspective drawing of the C_2 *cis*-$\mathrm{W_2Cl_4(NHBu^n)_2(PMe_3)_2}$ (**3b**) molecule. Atoms are represented by thermal ellipsoids at the 40% probability level. Carbon atoms are shown as spheres of arbitrary radius.

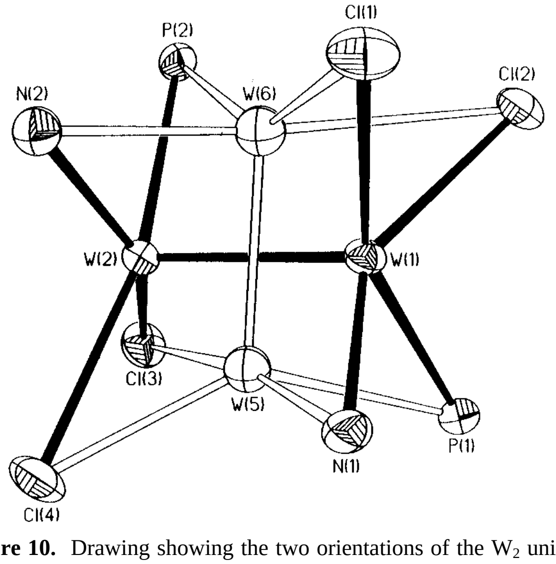

Figure 10. Drawing showing the two orientations of the $\mathrm{W_2}$ unit for the C_2 *cis*-$\mathrm{W_2Cl_4(NHBu^n)_2(PMe_3)_2}$ (**3a**) molecule.

Table 4. Selected Bond Distances (Å) and Angles (deg) for *cis*-$\mathrm{W_2Cl_4(NHPr^n)_2(PMe_3)_2}$ (**2**) and *cis*-$\mathrm{W_2Cl_4(NHBu^n)_2(PMe_3)_2}$ (**3a**,**b**)

	2	**3a**[a]	**3b**
W(1)−W(2)	2.3170(6)	2.3162(9)	2.3147(5)
W(1)−P(1)	2.512(2)	2.495(4)	2.506(3)
W(2)−P(2)		2.507(5)	2.506(2)
W(1)−N(1)	1.900(7)	1.91(1)	1.902(8)
W(2)−N(2)		1.90(1)	1.912(8)
W(1)−Cl(1)	2.381(2)	2.383(4)	2.385(2)
W(2)−Cl(4)		2.393(4)	2.402(2)
W(1)−Cl(2)	2.433(2)	2.418(4)	2.425(2)
W(2)−Cl(3)		2.416(4)	2.428(2)
P(1)−W(1)−N(1)	85.7(2)	86.1(4)	86.1(3)
P(1)−W(1)−Cl(1)	159.97(9)	159.1(2)	159.34(9)
P(1)−W(1)−Cl(2)	80.16(9)	80.3(2)	80.20(9)
N(1)−W(1)−Cl(1)	97.6(2)	97.0(4)	96.8(3)
N(1)−W(1)−Cl(2)	144.7(2)	145.3(5)	146.3(2)
Cl(1)−W(1)−Cl(2)	86.01(9)	85.8(2)	86.34(8)
W(2)−W(1)−P(1)	96.43(6)	96.2(1)	96.35(6)
W(2)−W(1)−N(1)	98.6(2)	98.1(4)	97.7(2)
W(2)−W(1)−Cl(1)	102.53(6)	103.9(1)	103.47(6)
W(2)−W(1)−Cl(2)	114.87(6)	115.0(1)	114.28(6)
P(2)−W(2)−N(2)		86.5(4)	86.1(2)
P(2)−W(2)−Cl(3)		79.6(2)	80.38(8)
P(2)−W(2)−Cl(4)		159.9(2)	160.25(8)
N(2)−W(2)−Cl(3)		145.0(4)	145.0(3)
N(2)−W(2)−Cl(4)		97.0(4)	97.0(2)
Cl(3)−W(2)−Cl(4)		86.5(2)	86.21(9)
W(1)−W(2)−P(2)		96.3(1)	96.36(6)
W(1)−W(2)−N(2)		98.7(4)	97.8(3)
W(1)−W(2)−Cl(3)		114.6(1)	115.54(6)
W(1)−W(2)−Cl(4)		102.8(1)	102.50(6)

[a] Distances and angles are the averages for the two independent molecules of the asymmetric unit.

compound **1** represents the first structurally characterized complex containing a $\mathrm{W_2Cl_4N_2P_2}$ core in a cis geometry with C_i symmetry. There is no disorder associated with the $\mathrm{W_2}$ unit in **1**. The W−W bond distance of 2.3066(6) Å is slightly shorter than those observed in other *cis*-$\mathrm{W_2Cl_4(NHR)_2(PR'_3)_2}$ compounds of the known type[1b,11] (Table 3). All other bonding parameters around the $\mathrm{W_2}$ core in **1** are similar to those encountered in the related $\mathrm{W_2}^{6+}$ complexes. The W−P and W−N distances are 2.497(2) and 1.912(7) Å, respectively, and Δ(W−Cl) is 0.034 Å. A salient structural feature is evident from the projection drawing shown in Figure 7a. It is clear that all atoms on the adjacent W atoms are related by center of symmetry and the four important torsional angles that define the $\mathrm{W_2Cl_4N_2P_2}$ unit are all less than 11° so that the conformation is essentially eclipsed. The two hydrogen bonds have a distance of 2.51 Å.

Compound **2** conforms to the monoclinic space group *I*2/*a* with four molecules per unit cell. Polymorphic compounds **3a**,**b** crystallize in the monoclinic space group No. 14, where we have used the settings $P2_1/c$ and $P2_1/n$ for **3a**,**b** respectively, with eight and four molecules (comprising two pairs of enantiomers) in the unit cells, respectively. Perspective views of the molecular structures of **2** and **3b** are shown in Figures 8 and 9, respectively. For **3a**, there are two independent molecules in the asymmetric unit. One molecular site shows no metal−metal disorder, while the other one has 0.944:0.056 metal−metal orientational disorder (Figure 10). Both orientations conform to the same isomer. The metrical parameters of these structures are summarized in Table 4. A few of the angular parameters

---

(11) (a) Bradley, D. C.; Hursthouse, M. B.; Powell, H. R. *J. Chem. Soc., Dalton Trans.* **1989**, 1537. (b) Cotton, F. A.; Yao, Z. *J. Cluster Sci.* **1994**, *5*, 11.

Table 5. Selected Torsion Angles (deg) for *cis*-$W_2Cl_4(NHPr^n)_2(PMe_3)_2$ (**2**) and *cis*-$W_2Cl_4(NHBu^n)_2(PMe_3)_2$ (**3a**,**b**)

	2		**3a**[a]	**3b**
P(1)−W(1)−W(1A)−Cl(2A)	16.63(9)	P(1)−W(1)−W(2)−Cl(3)	15.9(2)	17.07(9)
N(1)−W(1)−W(1A)−Cl(1A)	11.8(2)	N(1)−W(1)−W(2)−Cl(4)	10.8(4)	12.2(3)
Cl(1)−W(1)−W(2)−N(1A)	11.8(2)	Cl(1)−W(1)−W(2)−N(2)	10.9(4)	12.2(2)
Cl(2)−W(1)−W(2)−P(1A)	16.63(9)	Cl(2)−W(1)−W(2)−P(2)	15.3(2)	17.34(9)

[a] Torsion angles are the averages for the two independent molecules of the asymmetric unit.

Table 6. Comparison of Selected Bond Distances (Å) for Five *cis*-$W_2Cl_4(NHR)_2(PMe_3)_2$ (R = Bu^t, Cy, Bu^s, Bu^n, Pr^n) Molecules with a C_2 Symmetry

R	W−W	$(W-P)_{av}$	$(W-N)_{av}$	$(W-Cl)_{av}$[a]	$(W-Cl)_{av}$[b]	ref
Bu^t	2.3267(6)	2.523(3)	1.911(9)	2.383(3)	2.425(3)	11b
Cy	2.3229(5)	2.512(2)	1.904(5)	2.389(2)	2.418(2)	1b
Bu^s	2.321(1)	2.500(3)	1.89(1)	2.377(3)	2.421(3)	1b
Bu^n[c]	2.3147(5)	2.506(3)	1.907(8)	2.394(2)	2.427(2)	this work
Pr^n	2.3170(6)	2.512(2)	1.900(7)	2.381(2)	2.433(2)	this work

[a] W−Cl bond trans to P. [b] W−Cl bond trans to N. [c] Data based on **3b**.

are also displayed in Table 5. Generally speaking, the structural features of **2** and **3** (**3a**,**b**) possess many similarities. The core structure of each has only C_2 symmetry and these molecules are therefore chiral. All of them maintain an essentially eclipsed geometry with retention of a strong N−H···Cl hydrogen bonding with the torsion angles involving the hydrogen-bonded atoms lying within the range 10.8−17.3° (Figure 7b).

To date, together with **2** and **3**, there are five structurally characterized examples of *cis*-$W_2Cl_4(NHR)_2(PMe_3)_2$ molecules of C_2 symmetry having different R groups (R = Bu^t, Cy, Bu^s, Bu^n, Pr^n).[1b,11] Table 6 compares numerically the important dimensions for these molecules. An examination of the M−L bond lengths for these compounds reveals some general and expected trends throughout the series: (i) An average W−N distance of ca. 1.90 Å represents a normal W−NH(R) bond length of formal bond order two. (ii) The W−P distance is that expected for *cis* isomer when compared to the W−P distances found in other W_2^{6+} complexes in a trans stereochemistry.[11] (iii) The average W−Cl distance, trans to N, is longer than that trans to P in each case (Δ(W−Cl) range, 0.029−0.052 Å). This is doubtless a manifestation of the structural trans influence order NHR > PMe_3, observed in many other systems.[1b,11]

Concluding Remarks

This report describes our recent success in observing in solution and even isolating an example of the previously unknown *cis* isomer of C_i symmetry for the $W_2Cl_4(NHR)_2(PR'_3)_2$ type molecules and presents the structure determined by X-ray crystallography for R = Et and R′ = Me. This second *cis* isomer is particularly interesting in view of the proposed internal flip mechanism for *cis*−*trans* isomerization of such molecules since it should be available by a unimolecular process entailing one internal flip. The basic strategy we adopted is to make use of the least sterically bulky amido substituents around the metal core so that the steric limitations on the products are relaxed as much as possible. The most important result of changing the amido groups to the smaller ones is such that the previously unknown *cis* isomer of C_i symmetry can be seen in solution and even, in one case, isolated.

On the other hand, the fact that *cis*−*trans* isomerization can occur, in theory, by a flip mechanism does not, of course, require that this be the only mechanism or even a viable one, for the process. Clearly, some mechanism entailing the initial dissociation of phosphine ligands cannot be ruled out at this stage.[1a] Although no quantitative data are available at present, qualitative studies of the isomerization process for $W_2Cl_4(NHEt)_2(PMe_3)_2$ in the presence of excess PMe_3 indicated that addition of free PMe_3 ligand did cause a slight but definite retardation in the rate of isomerization (t_∞ changes from 5 to 8 h, where t_∞ is the time for complete disappearance of the *trans* isomer). The effect became insignificant upon further increase in [PMe_3], from which we suggest that suppression of a dissociative mechanism leaves a nondissociative one. The only type of nondissociative path we can imagine must involve flipping. These matters remain the subject of future work and further consideration.

Acknowledgment. We are grateful to the National Science Foundation for support.

Supporting Information Available: Four X-ray crystallographic files, in CIF format, are available. Access information is given on any current masthead page.

IC9700361